Inorganic Chemistry

Article

pubs.acs.org/IC

Field Supported Slow Magnetic Relaxation in a Mononuclear Cu(II) Complex

Roman Boča,* Cyril Rajnák, Ján Titiš, and Dušan Valigura

Department of Chemistry, Faculty of Natural Sciences, University of SS. Cyril and Methodius, 917 01 Trnava, Slovakia

Supporting Information

ABSTRACT: A mononuclear hexacoordinate Cu(II) complex shows a field induced slow magnetic relaxation that is not facilitated by an energy barrier to spin reversal due to the zero-field splitting. Two relaxation channels were found: the magnetic field strongly supports the low-frequency relaxation path with a relaxation time as long as $\tau = 0.8$ s at $T = 1.9$ K and $B = 1.5$ T. The mechanism of the relaxation at low temperature involves the dominant Raman process for this $S = 1/2$ spin system along with a temperature-independent term belonging to a quantum tunneling.

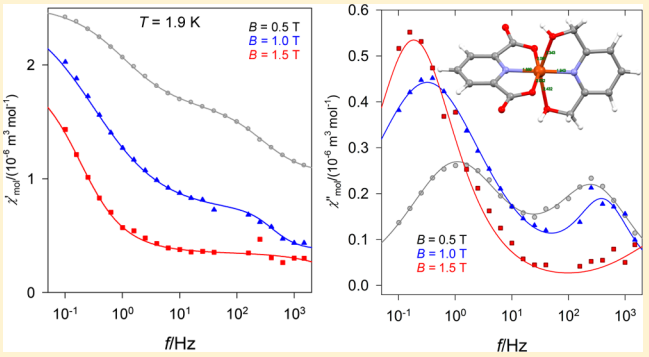

INTRODUCTION

Unlike the classical magnetic materials, such as ferrites widely used in many branches of technique and everyday life, a new class of magnetic materials exclusively based on molecular entities has been discovered and it is a subject of intense investigation at present. These single-molecule magnets and/or single-ion magnets (SMMs, SIMs) exhibit a slow magnetic relaxation that means that the magnetic information borne by a single molecule survives for a long enough time (typical extrapolated relaxation time is $\tau_0 \sim 10^{-6}$ s).

The SMMs were originally identified among polynuclear complexes of Mn(III)-Mn(IV) and Fe(III) containing 12 or 8 metal centers which dates to the early 90s.[1,2] In a couple of years, many other polynuclear complexes based upon the transition metal atoms were studied as SMMs including many heteronuclear "clusters". In the next stage, the center of attention was forwarded to lanthanides, among which the polynuclear and mononuclear Dy(III) complexes dominated. In parallel, 3d−4f complexes were widely studied, such as Cu(II)-Dy(III) and many others.[3,4]

In the last stage, research returned to mononuclear complexes of the first transition metal series. It is worth noting that these SMMs were identified for Cr(II), Mn(III), Fe(III), Fe(II), Fe(I), Co(II), and Ni(II) systems.[5−7] No report exists about the SMM properties of mononuclear Cu(II) complexes so far, though some Ni(I), V(IV), and Mn(IV) complexes were classified as SMMs.[8−10] This is probably given by the mental barrier that SMMs require large magnetic anisotropy expressed by a negative axial zero-field splitting parameter $D < 0$. Such a parameter is undefined for the $S = 1/2$ spin systems so that we cannot speak about the barrier to spin reversal $\Delta = |D|S^2$ that hinders the magnetic relaxation. Herein, we are reporting about a missing puzzle among first-transition metal single-molecule magnets that is a mononuclear Cu(II) complex showing slow magnetic relaxation.

Recently, the mononuclear complex [Ni(*pydca*)(*dmpy*)]·H_2O was identified as the first SMM containing the Ni(II) central atom (*pydca* = pyridine-2,6-dicarboxylato, *dmpy* = 2,6-dimethanolpyridine).[11] Magnetic data taken in a static magnetic field (temperature dependence of the magnetic susceptibility and field dependence of the magnetization) show a rather large magnetic anisotropy with a considerable value of the axial zero-field splitting parameter $D/hc = -12.7$ cm^{-1}. This was thought as a prerequisite of the SMM behavior. The AC susceptibility data in the small oscillating magnetic field confirms that this system is a field-induced SMM with two relaxation channels. Motivated by this result, we probed the copper(II) analogue [Cu(*pydca*)(*dmpy*)]·0.5H_2O, hereafter **1**, for the SMM properties. Its molecular structure is viewed in Figure 1. Structure details are contained in the Supporting Information (SI).

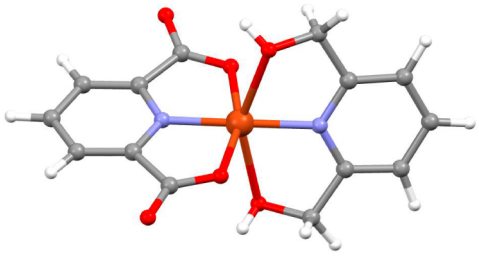

Figure 1. Molecular structure of **1**.

Received: October 21, 2016
Published: January 9, 2017

DOI: 10.1021/acs.inorgchem.6b02535
Inorg. Chem. 2017, 56, 1478−1482

EXPERIMENTAL SECTION

The complex **1** was synthesized according to the published procedure, and the standard analytical verification confirms the identity and purity of the powder material. The X-ray structure of [Cu(*pydca*)(*dmpy*)] was described elsewhere and was deposited in the CCDC as KOLHUO.[12] However, another structure determination done at r.t. showed a different space group and different cell parameters, though the molecular units are almost identical; this is deposited under the code VARDUP.[13] The present sample **1** refers to the [Cu(*pydca*)-(*dmpy*)]·0.5H_2O, as confirmed by the structure redetermination at T = 100 K. The identity of the powder material used for magnetic measurements was confirmed by the X-ray powder diffraction patterns (see the SI).

DC magnetic data were taken with the SQUID magnetometer (MPMS-XL7, QuantumDesign) using the RSO mode of detection at B_{DC} = 0.5 T. The sample (50.27 mg) was encapsulated in diamagnetic gelatin made sample holders. The molar magnetic susceptibility was corrected to the underlying diamagnetism and presented in the form of the effective magnetic moment. The magnetization data were taken at T = 2.0 and 4.6 K until B_{DC} = 7.0 T, and they are presented in the form of magnetization per formula unit per Bohr magneton, $M_1 = M_{mol}/(N_A\mu_B)$.

AC susceptibility data were taken with the same hardware at the oscillating field B_{AC} = 0.38 mT for 22 frequencies ranging between f = 0.1 and 1500 Hz. In these measurements, an external magnetic field B_{DC} = 0.5, 1.0, and 1.5 T was applied.

For quantum chemical calculations, the *ab initio* method was chosen, namely, the complete active space self-consistent field (CASSCF), followed by the second-order N-electron valence perturbation theory (NEVPT2).[14] An active space in which nine electrons are distributed into the five copper d-orbitals (CAS(9,5)) was employed along with the ZORA-TZV basis set for all elements. In the CASSCF procedure, the orbitals were optimized for the average of 5 doublet roots (^{2}D term of the free Cu(II)).

RESULTS

Magnetic data taken in a static magnetic field (DC data) show a typical behavior for the S = 1/2 spin system and could be considered as rather boring since the Curie−Weiss law holds true. A simultaneous analysis of the susceptibility and magnetization data yields $g_x = g_y$ = 2.051, g_z = 2.385, a small correction to the molecular field effective at low temperature (zj/hc = −0.087 cm^{-1}), and some temperature-independent magnetism χ_{TIP} = 0.24 × 10^{-9} m^3 mol^{-1} (SI units are employed). This matches an earlier report on electron spin resonance of a polycrystalline sample with g_x = 2.139, g_y = 2.040 and g_z = 2.238 and/or g_x = 2.121, g_y = 2.007 and g_z = 2.262.[12,13]

Verification of the experimental findings has been made by *ab initio* calculations based on the X-ray diffraction-determined structure. The g values were calculated using the effective Hamiltonian formalism yielding g_1 = 2.055, g_2 = 2.095, g_3 = 2.364, and g_{iso} = 2.172.

New information comes from the AC susceptibility measurements. They were conducted first at low temperature T = 2.0 K for four frequencies of the oscillating field in dependence on the external magnetic field B_{DC} = 0−1.7 T (Figure 2). It can be seen that the out-of-phase component χ'' at the zero field is silent; however, with increasing field, χ'' passes through a maximum between 0.5 and 1.0 T. This behavior indicates that **1** exhibits the field induced slow magnetic relaxation. (A scattering of the data points in Figure 2 is probably due to a weak magnetic response of the S = 1/2 spin system for B_{AC} = 0.38 mT.)

A frequency dependence of the AC susceptibility components at a constant temperature is presented in Figure 3. Two peaks are recognized at the χ'' vs f dependence: the low-frequency (LF) peak appears around 1 Hz, whereas the high-frequency (HF) peak exists around 250 Hz.

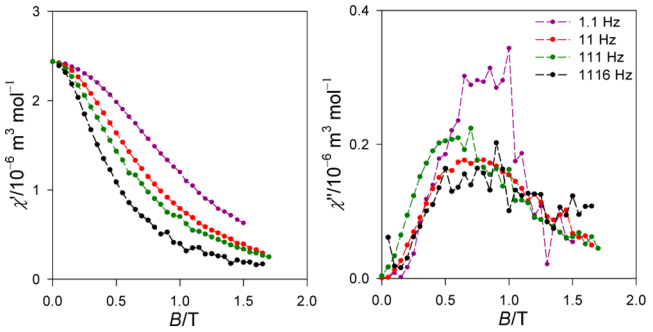

Figure 2. In-phase χ' and out-of-phase χ'' molar susceptibility (SI units) for **1** in dependence upon external magnetic field at T = 2.0 K. Lines serve as a guide for eyes.

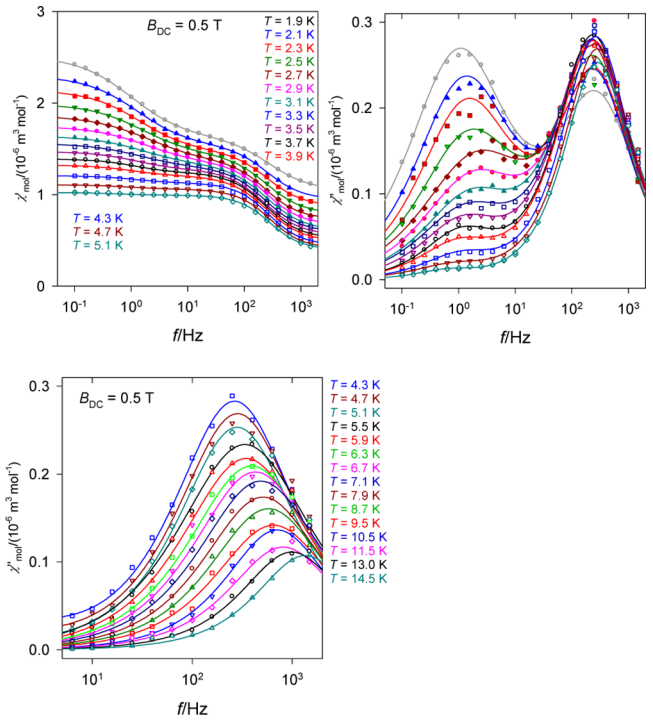

Figure 3. Frequency dependence of the AC susceptibility components for **1** at B_{DC} = 0.5 T. Left: the in-phase component; right: the out-of-phase component; bottom: the out-of-phase component for higher temperature. Lines: fitted with a two-set Debye model.

The experimental data of the AC susceptibility components (22 in-phase and 22 out-of-phase points) was processed by fitting to a two-set Debye model that contains 7 free parameters: the adiabatic susceptibility χ_S, two isothermal susceptibilities χ_{T1} and χ_{T2}, the corresponding distribution parameters α_1, α_2, and the relaxation times τ_1 and τ_2 referring to two branches of the relaxation. The final parameters (see the SI) were used in reconstructing the interpolation and extrapolation lines that are drawn in Figure 3 and tightly passing through the experimental points. The quality of the fitting procedure is evaluated: (i) by the discrepancy factors for the susceptibility components $R(\chi')$ and $R(\chi'')$, respectively; (ii) the standard deviation for each optimized parameter σ_p; (iii) a smooth variation of each parameter with temperature.

DOI: 10.1021/acs.inorgchem.6b02535
Inorg. Chem. 2017, 56, 1478−1482

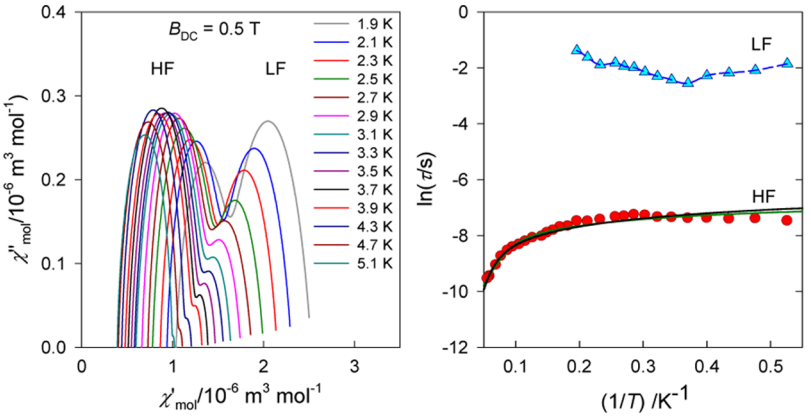

Figure 4. The fitted AC susceptibility data for **1** at B_{DC} = 0.5 T. Left: Argand diagram (fixed temperature); lines: calculated upon fitted parameters. Right: Arrhenius-like plot; full lines: fitted by model A (Orbach + direct + tunneling, green line) and B (Raman + direct + tunneling, black line).

Table 1. Relaxation Parameters for the HF Branch of 1[a]

	B_{DC} = 0.5 T, model A	B_{DC} = 0.5 T, model B	B_{DC} = 1.0 T, model A	B_{DC} = 1.0 T, model B
U/k_B/K	58.6(52)		62.7(69)	
τ_0/s	4.5(11) × 10^{-6}		2.4(11) × 10^{-6}	
A/T^{-m} K^{-1} s^{-1}, m = 4	4.2(5) × 10^3	5.2(4) × 10^3		
C/K^{-n} s^{-1}, n = 5		4.3(2) × 10^{-3}		8.6(3) × 10^{-3}
D_t/s^{-1}	7.8(16) × 10^2	5.3(14) × 10^2	1.9(1) × 10^3	1.9(1) × 10^3
discrepancy factor R	0.047	0.056	0.12	0.12

[a]Standard deviations are in parentheses. Correlation matrix in the SI confirms that the parameters are not mutually correlated except U and τ_0 for the Orbach process.

The Argand diagram for the fixed temperature is drawn in Figure 4, left. It consists of two distorted and overlapping arcs. The frequencies of the maxima (or better directly the fitted relaxation times) enter the Arrhenius-like plot that is shown in Figure 4, right. It can be seen that the HF branch behaves with expectations: at very low temperature, it is nearly constant, and at increasing temperature, the relaxation time decreases. However, the LF branch shows an unexpected increase of the relaxation time τ_1 on temperature propagation; above some limit, it cannot be evaluated since the χ_{T1} value (height of the LF peak) tends to vanish.

The HF branch has been further processed by fitting to the extended relaxation equation

$$\tau^{-1} = \tau_0^{-1} \exp(-U/k_BT) + AB^mT + CT^n + D_t \qquad (1)$$

that reflects Orbach, direct, Raman, and quantum tunneling relaxation processes.[15] This complex formula refers to various types of the interactions between spins and lattice vibrations (phonons) contributing to the spin−lattice relaxation. In the Orbach process, absorption of a phonon is followed by phonon emission and relaxation from an excited state. In the Raman process, relaxation proceeds through a virtual state. The direct process involves relaxation from $-M_S$ to $+M_S$ states with emission of a single lattice phonon. Quantum tunneling relaxation is facilitated by the transverse anisotropy of the system. Each of these processes is active in the different temperature region and can be examined using a very limited data.[16] The involvement of the D_t parameter is essential when the relaxation time becomes independent of temperature.

The fitting procedure with omission of either Raman (model A) or Orbach (model B) processes gave the relaxation parameters as listed in Table 1. The Orbach process requires a presence of the (effective) energy barrier U originating in the zero-field splitting of the ground term, which is not the case of the Cu(II) systems. The chromophores around the Cu1 and Cu2 centers are asymmetric (point group C_1) with all metal−ligand distances differing from each other. Thus, the ground electronic term 1^2A_1 is followed by its counterpart 2^2A_1 arising from the Jahn−Teller splitting of the (hypothetical) octahedral term ^2E_g. The virtual barrier to spin reversal U spans the expected range, and the extrapolated relaxation time τ_0 is also typical for SMMs of this class, e.g., mononuclear Co(II) complexes.[5−7]

The fitting procedure for the HF branch, however, is only partly successful. A detailed inspection shows that the low-temperature data exhibit an unexpected decrease of the relaxation time on cooling below 3.5 K (see the SI for a better resolution). The origin of this effect remains unmodeled so far, though a phenomenological "inverse" term $\tau^{-1} = E_iT^{-k}$ (k = 1−3) improves the fit of the low-temperature relaxation rate. It is worth mentioning that such a low-temperature behavior is evident also for the V(IV) SMM.[9]

A mapping of the AC susceptibility components as functions of the frequency for a set of external magnetic fields B_{DC} = 1.0, and 1.5 T is deposited in the SI. The data are more scattered relative to the scans at B_{DC} = 0.5 T probably due to a lower stability of the external field. Again, two relaxation channels are detected. An increase of the external magnetic field to B_{DC} = 1.0 T causes that the height of the LF peak at χ'' increases, and at B_{DC} = 1.5 T, this peak dominates. Moreover, the maximum of the LF peak moves to lower frequencies so that the relaxation time at T = 1.9 K is τ = 0.156, 0.483, and 0.842 s at B_{DC} = 0.5, 1.0, and 1.5 T, respectively. On passing from B_{DC} = 0.5 to 1.5 T, the peak positions of the HF branch move to higher frequencies and consequently the relaxation times are shortened. The Arrhenius-like plot for the HF branch displays

DOI: 10.1021/acs.inorgchem.6b02535
Inorg. Chem. 2017, 56, 1478−1482

an usual behavior, and thus a fitting to the extended relaxation eq 1 is facilitated also for B_{DC} = 1.0 T. Again, a detailed inspection to the low-temperature data indicates an unprecedented decrease of ln τ(HF) at the lowest temperatures of the data acquisition.

DISCUSSION

The D and E (axial and orthorhombic zero-field splitting parameters) enter the spin-Hamiltonian formalism where they parametrize the spin−spin interaction for systems with $S > 1/2$, whereas the g-tensor components parametrize the Zeeman (spin-magnetic field) interaction.[17] Though the D parameter cannot be assigned to mononuclear copper(II) complexes, these are well-known as anisotropic systems showing at least two distinct $g_z \neq g_x$ values well seen in the EPR spectra of an axial type. Thus, even in the absence of the zero-field splitting, there exists a magnetic anisotropy. This is visualized by a 3D diagram of the magnetization per particle $M(x, y, z)$ calculated for an $S = 1/2$ system at T = 2.0 K and B = 1.0 T (Figure 5)

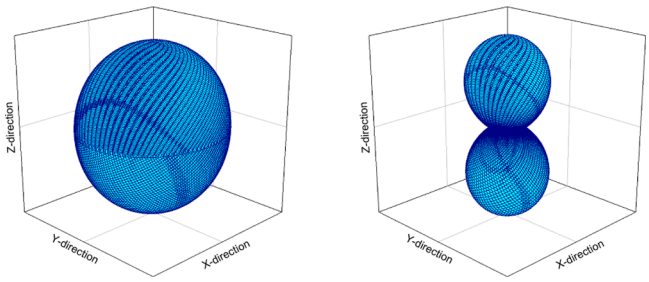

Figure 5. 3D diagram of the magnetization $M(z, y, z)$ for B = 1.0 T and T = 2.0 K. Left: the $S = 1/2$ system with anisotropic g-factors. Right: $S = 1$ system with all g = 2.0 and $D/hc = -10$ cm^{-1} (easy axis magnetic anisotropy along the z-axis).

resembling a prolate ellipsoid. With a higher difference $g_z - g_x$, the eccentricity of the ellipsoid increases. This picture is different from the case of $S = 1$ with negative axial zero-field splitting (easy axis system, resembling a "barbell").

The spin-Hamiltonian formalism predicts a constraint $D = \lambda(g_z - g_x)/2$, where λ is the spin−orbit splitting parameter within the ground term. Using the EPR data (g_x = 2.139, g_y = 2.040, g_z = 2.238) and λ/hc = 830 cm^{-1}, one gets the asymmetry parameter $D_{ap}/hc = -61.6$ cm^{-1}. This value does not refer to any energy gap for the $S = 1/2$ spin system, but it can be exploited in quantifying the magnetic anisotropy.

The relaxation time depends upon temperature, and on heating, it normally becomes shorter. Therefore, for comparison, an extrapolated relaxation time τ_0 used to be presented (this is a hypothetical relaxation time at infinite temperature that can be obtained by an extrapolation). Typically, $\tau_0 \sim 10^{-6}$ s is characteristic for SMMs, though lower or higher values were also reported. These values are by several orders of magnitude shorter than the relaxation time for spin glasses (typically $\tau_0 \sim 10^{-20}$ s).[18]

A detailed inspection to the magnetic data in Figure 3 shows that there is a slight asymmetry of the low-frequency peak at χ'' that cannot be covered by the distribution parameter α_1 itself. On heating, this peak vanishes progressively. Its position moves to higher frequencies and then returns back to lower frequencies. Such a feature has been detected for a number of mononuclear Co(II) and also in Ni(II) complexes showing two relaxation channels. Quantitatively, a peak maximum at ca. 1 Hz implies τ(LF) = $1/(2\pi f''_{max}) \sim 0.16$ s; this value is by 4 orders of magnitude longer than values typical for SMMs.

The positions of high-frequency peaks at χ'' lie at $f \sim 666$ Hz, and they are almost temperature independent in the interval of 1.9−3.9 K, giving rise to the relaxation time τ(HF) $\sim 6 \times 10^{-4}$ s (at the same conditions, B_{DC} = 0.5 T).

The appearance of the LF relaxation path is attributed to the existence of intermolecular interactions always present in small molecular systems with aromatic rings. These can form "finite oligomers" (finite chains, plates, blocks) with coherence length depending upon temperature. For a high enough temperature, only the monomeric units are subjected to the slow relaxation (HF path), whereas the LF path escapes progressively with temperature as the oligomers disintegrate into monomers.

The intermolecular origin of the LF relaxation path can be examined by doping experiments. Doping of Cu(II) into the Zn(II) matrix meets an obstacle that the magnetic response is too low and the data are scattered even at the maximum setup of B_{AC} = 0.38 mT. A doping experiment has been done for the Ni analogue of **1** which possesses a similar structure and similar AC susceptibility response with two relaxation channels.[7] For the pure Ni(II) system, the low-frequency mole fraction varies as x_{LF} = 0.28, 0.18, and 0.12 for T = 1.9, 2.3, and 2.7 K at B_{DC} = 0.2 T. At the same conditions, the Ni:Zn complex with 55% of Ni possesses x_{LF} = 0.20, 0.13, and 0.09 for the same set of temperatures. In other words, the yield of the LF branch was reduced as an effect of the doping, which points to the intermolecular nature of the LF relaxation channel.

Worth noting is also the influence of the external magnetic field for **1**: x_{LF} = 0.61, 0.53, and 0.46 for T = 1.9, 2.3, and 2.7 K at B_{DC} = 0.5 T. At B_{DC} = 1.5 T, there is x_{LF} = 0.82, 0.78, and 0.75 for the same set of temperatures. Such an expressive preference of the LF relaxation channel in **1** is different from other SMMs represented by Co(II) complexes.

On the basis of doping experiments, the intermolecular nature of the LF relaxation channel has also been explored for a heptacoordinate Co(II) complex with $D > 0$.[13] The extracted value of $U/k_B \sim$ 50−55 K for the HF channel is rather unaffected by the degree of doping, which confirms an intramolecular nature of this relaxation. The magnetic field raises the efficiency of the LF relaxation path (measured by x_{LF}), which points to its intermolecular nature supported by the magnetic field. Moreover, the relaxation time is prolonged with increasing magnetic field.

Some groups argue that the hyperfine interaction of the ^{59}Co nuclear spin $I = 7/2$ assists in the slow magnetic relaxation in Co(II) complexes.[19−21] The Co(II) systems with $S = 3/2$ and large D values can be considered as an effective $S^* = 1/2$ system at low temperature when only one Kramers doublet is populated. The transition with $\Delta M_{S^*} = \pm 1/2$ is phonon-forbidden. However, the electron−nuclear hyperfine interaction generates 16 sublevels $|S^*, I, M_{S^*}, M_I\rangle$, among which 8 transitions are allowed at the applied field. This could be the case of Cu(II) complexes with $S = 1/2$ since both natural isotopes ^{63}Cu and ^{65}Cu possess $I = 3/2$. The difference with respect to Co(II) is the existence of 8 hyperfine levels only with four allowed transitions for $\Delta M_S = \pm 1$ and $\Delta M_I = 0$. However, for ^{61}Ni with a natural abundance of only 1.2%, $I = 3/2$ holds true so that the above argument is problematic to accept for Ni(II) containing SMMs, particularly for the Ni(II) analogue of **1**.

DOI: 10.1021/acs.inorgchem.6b02535
Inorg. Chem. 2017, 56, 1478−1482

To this end, essential is the Raman process of the relaxation for the Cu(II) $S = 1/2$ system, similar to the case of Co(II) effective spin $S^* = 1/2$.[20]

CONCLUSIONS

The system under study refers to the mononuclear Cu(II) molecular complex where the slow magnetic relaxation was observed in an applied DC magnetic field. There is no energy barrier to spin reversal due to the zero-field splitting in this system. There are two channels of the slow magnetic relaxation: the low-frequency around 1 Hz, and the high-frequency close to 1000 Hz. The external magnetic field influences the characteristics of the magnetic relaxation dramatically: with increasing field, the relaxation time is prolonged, and at $T = 1.9$ K and $B_{DC} = 1.5$ T, it is as slow as $\tau = 0.8$ s.

ASSOCIATED CONTENT

Supporting Information

The Supporting Information is available free of charge on the ACS Publications website at DOI: 10.1021/acs.inorgchem.6b02535.

Details about the crystal and molecular structure (CCDC 1494077) and magnetic data analysis (PDF)

Crystallographic data for **1** (CIF)

AUTHOR INFORMATION

Corresponding Author

*E-mail: roman.boca@ucm.sk.

ORCID

Roman Boča: 0000-0003-0222-9434

Dušan Valigura: 0000-0001-7834-7395

Notes

The authors declare no competing financial interest.

ACKNOWLEDGMENTS

Slovak grant agencies (VEGA 1/0522/14, VEGA 1/0534/16, APVV-14-0078) are acknowledged for the financial support. The authors are thankful to Prof. Ján Moncol′ and Dr. M. Puchoňová (Slovak University of Technology, Bratislava) for performing the X-ray structure determination and XPD of **1**.

REFERENCES

(1) Sessoli, R.; Gatteschi, D.; Caneschi, A.; Novak, M. A. Magnetic bistability in a metal-ion cluster. *Nature* **1993**, *365*, 141−143.

(2) Villain, J.; Hartman-Boutron, F.; Sessoli, R.; Rettori, A. Magnetic-relaxation in big magnetic molecules. *Europhys. Lett.* **1994**, *27*, 159−164.

(3) Gatteschi, D.; Sessoli, R.; Villain, J. *Molecular Nanomagnets*; Oxford University Press: Oxford, U.K., 2006.

(4) Winpenny, R. Single-molecule magnets and related phenomena. *Struct. Bonding* **2006**, *122*, 1.

(5) Craig, G. A.; Murrie, M. 3d single ion magnets. *Chem. Soc. Rev.* **2015**, *44*, 2135−2147 and references therein.

(6) Gomez-Coca, S.; Aravena, D.; Morales, R.; Ruiz, E. Large magnetic anisotropy in mononuclear metal complexes. *Coord. Chem. Rev.* **2015**, *289−290*, 379−392 and references therein.

(7) Frost, J. M.; Harriman, K. L. M.; Murugesu, M. The rise of 3-d single-ion magnets in molecular magnetism: towards materials from molecules? *Chem. Sci.* **2016**, *7*, 2470−2491 and references therein.

(8) (a) Lin, W.; Bodenstein, T.; Mereacre, V.; Fink, K.; Eichhofer, A. Field-Induced Slow Magnetic Relaxation in the Ni(I) Complexes $[NiCl(PPh_3)_2]\cdot C_4H_8O$ and $[Ni(N(SiMe_3)_2)(PPh_3)_2]$. *Inorg. Chem.* **2016**, *55*, 2091−2100. (b) Poulten, R. C.; Page, M. J.; Algarra, A. G.; Le Roy, J. L.; Lopez, I.; Carter, E.; Llobet, A.; Macgregor, S. A.; Mahon, M. F.; Murphy, D. M.; Murugesu, M.; Whittlesey, M. K. Synthesis, Electronic Structure, and Magnetism of $[Ni(6\text{-}Mes)_2]^+$: A Two-Coordinate Nickel(I) Complex Stabilized by Bulky N-Heterocyclic Carbenes. *J. Am. Chem. Soc.* **2013**, *135*, 13640−13643.

(9) Atzori, M.; Tesi, L.; Morra, E.; Chiesa, M.; Sorace, L.; Sessoli, R. Room-Temperature Quantum Coherence and Rabi Oscillations in Vanadyl Phthalocyanine: Toward Multifunctional Molecular Spin. Qubits. *J. Am. Chem. Soc.* **2016**, *138*, 2154−2157.

(10) Ding, M.; Cutsail, G. E., III; Aravena, D.; Amoza, M.; Rouzières, M.; Dechambenoit, P.; Losovyj, Y.; Pink, M.; Ruiz, E.; Clérac, R.; Smith, J. M. A low spin manganese(IV) nitride single molecule magnet. *Chem. Sci.* **2016**, *7*, 6132−6140.

(11) Miklovič, J.; Valigura, D.; Boča, R.; Titiš, J. A field induced single-molecule magnet showing two slow relaxation processes. *Dalton Trans.* **2015**, *44*, 12484−12487.

(12) Koman, M.; Melnik, M.; Moncol′, J. Crystal and molecular structure of copper(II) (pyridine-2,6-dicarboxylato)(2,6-dimethanolpyridine). *Inorg. Chem. Commun.* **2000**, *3*, 262−266.

(13) Tamer, O.; Sariboga, B.; Ucar, I.; Buyukgungor, O. Spectroscopic characterization, X-ray structure, antimicrobial activity and DFT calculations of novel dipicolinate copper(II) complex with 2,6-pyridinedimethanol. *Spectrochim. Acta, Part A* **2011**, *84*, 168−177.

(14) Neese, F. The ORCA program system. *Rev. Comput. Mol. Sci.* **2012**, *2*, 73.

(15) Carlin, R. L. *Magnetochemistry*; Springer: Berlin, 1986; p 49.

(16) Harman, W. H.; Harris, T. D.; Freedman, D. E.; Fong, H.; Chang, A.; Rinehart, J. D.; Ozarowski, A.; Sougrati, M. T.; Grandjean, F.; Long, G. J.; Long, J. R.; Chang, C. J. Slow Magnetic Relaxation in a Family of Trigonal Pyramidal Iron(II) Pyrrolide Complexes. *J. Am. Chem. Soc.* **2010**, *132*, 18115.

(17) Boča, R. Magnetic functions beyond the spin Hamiltonian. *Struct. Bonding (Berlin, Ger.)* **2006**, *117*, 1−226.

(18) Midosh, J. A. *Spin Glasses: An Experimental Introduction*; Taylor & Francis: London, 1993.

(19) Habib, F.; Korobkov, I.; Murugesu, M. Exposing the intermolecular nature of the second relaxation pathway in a mononuclear cobalt(II) single-molecule magnet with positive anisotropy. *Dalton Trans.* **2015**, *44*, 6368−6373.

(20) Gómez-Coca, S.; Urtizberea, A.; Cremades, E.; Alonso, P. J.; Camón, A.; Ruiz, E.; Luis, F. Origin of slow magnetic relaxation in Kramers ions with non-uniaxial anisotropy. *Nat. Commun.* **2014**, *5*, 4300.

(21) Vaidya, S.; Tewary, S.; Kumar Singh, S.; Langley, S. K.; Murray, K. S.; Lan, Y.; Wernsdorfer, W.; Rajaraman, G.; Shanmugam, M. What Controls the Sign and Magnitude of Magnetic Anisotropy in Tetrahedral Cobalt(II) Single-Ion Magnets? *Inorg. Chem.* **2016**, *55*, 9564−9578.

DOI: 10.1021/acs.inorgchem.6b02535
Inorg. Chem. 2017, 56, 1478−1482